Electronic Structure of Ni Coordination Complexes and [NiFe] Hydrogenase by Resonant Inelastic X-ray Scattering

P. Glatzel,[1] U. Bergmann,[1,2] S. Stepanov,[3] S. P. Cramer[1,2]
[1]Department of Applied Science, University of California, Davis, CA, U.S.A.
[2]Lawrence Berkeley National Laboratory (LBNL), Berkeley, CA, U.S.A.
[3]Biophysics Collaborative Access Team (Bio-CATS), Advanced Photon Source, Argonne National Laboratory, Argonne, IL, U.S.A.

Introduction

In resonant inelastic x-ray scattering (RIXS) or x-ray resonance Raman spectroscopy (XRRS), the fluorescence decay of a resonantly excited (intermediate) state is recorded by using a spectrometer with an energy bandwidth comparable or smaller than the lifetime broadening of the intermediate state [1]. We performed *1s2p* RIXS spectroscopy on Ni coordination complexes and [NiFe] hydrogenase at Bio-CATS beamline 18-ID [2].

In the two-step model for *1s2p* RIXS, an incident photon with energy Ω promotes a *1s* electron into an unoccupied molecular orbital. A *2p* electron fills the *1s* vacancy and emits a photon with energy ω. Although both incident and emitted photons lie in the hard x-ray range (>5 keV), the final states of the system exhibit the same *2p* vacancy encountered in L-edge soft x-ray spectroscopy. This is illustrated for a *"1s → 3d"* resonance in Fig. 1. A theoretical description for *1s2p* RIXS employs the same Kramers-Heisenberg equation used to describe the UV-visible RRS [3]. The intermediate state with a *1s* core hole is reached from the electronic ground state via the dipole or quadrupole operator. The decay of the *1s* hole occurs via the dipole operator into the final state with a *2p* vacancy.

Several intermediate and final states can be reached. The splittings and relative intensities of the transitions between the different states contain chemical information about the system under investigation. This information can be displayed in a contour plot, where the two axes are the incident energy Ω and the energy transfer Ω - ω. The energy transfer Ω - ω (final state energy) scale corresponds with the excitation energy in L-edge spectra (Fig. 1), and we obtain L_3 ($2p_{3/2}$) and L_2 ($2p_{1/2}$)-like spectra by projections along constant incident energy Ω.

Methods and Materials

The RIXS spectra were recorded at the Bio-CAT beamline [4]. The incident beam monochromator used a pair of Si(400) crystals, and the energy bandwidth at 8330 eV was 1.0 eV. Radiation damage studies were performed on each sample. The fluorescence spectrometer for the current experiments used three 8.9-cm-diameter Si(620) analyzer crystals. The fluorescence spectrometer energy bandwidth was approximately 0.8 eV at 7478 eV[5]. For the Ni samples, see Ref. 2.

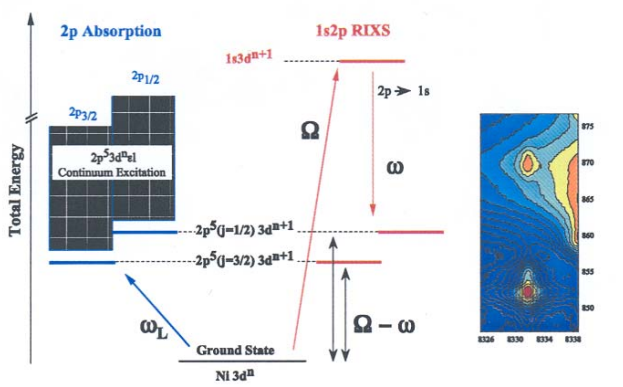

FIG. 1. Energy scheme for 1s2p RIXS compared to L-edge absorption spectroscopy. A 1s2p RIXS contour plot for NiF_2 is shown as an example, and the two line plots that we extract from the contour plots are illustrated. The photon energies are denoted ω_L (L edge), Ω (K edge), and ω (inelastically scattered).

Results and Discussion

Figure 2 illustrates the properties of *1s2p* RIXS for Ni in various spin and oxidation states [3]. We focus on the "pre-edge" excitation region that involves the lowest unoccupied molecular orbitals and on final states with $2p_{3/2}$ vacancies (L_3 edge). In these contour plots, the intensities (on logarithmic scales) are expressed as different colors. The resonant excitations appear as islands in the plots, with tails extending parallel to the Ω and Ω - ω axes. The structures that stretch diagonally in the plots indicate the background mainly from excitations of a *1s* electron into the continuum.

By traversing the contour plots along lines of constant Ω - ω, one obtains excitation spectra for constant final state energy, as shown in Fig. 3. The weak *1s → 3d* resonances are now separated from the strong dipole allowed transitions at higher energies. The shifts of the

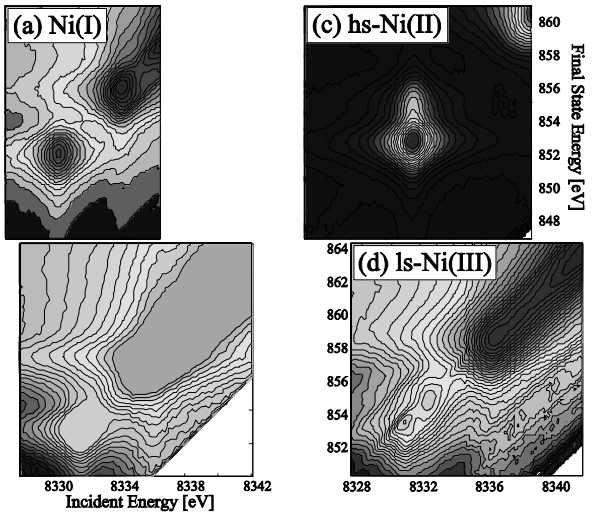

FIG. 2. Contour plots for Ni coordination complexes: (a) Ni(I) in [PhTt^{tBu}]NiCO, Ni(II). (b) Low-spin (ls) in (Ph$_4$As)$_2$Ni(S$_2$C$_2$(CF$_3$)$_2$)$_2$, Ni(II). (c) High-spin (hs) in NiF$_2$. (d) Ni(III) low-spin in [Ni(η^4-DEMAMPA-DCB)]$^-$.

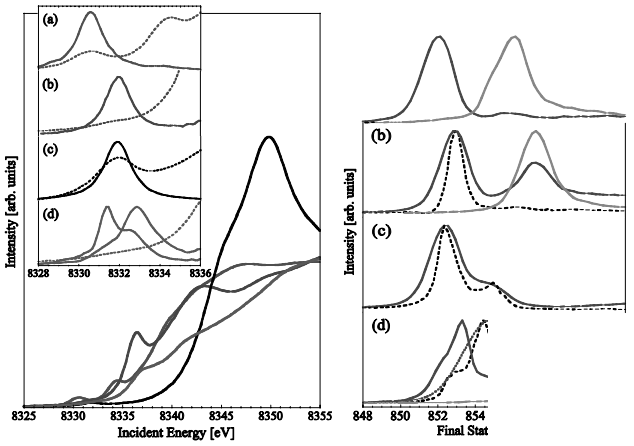

FIG. 3. Left panel: K-edge absorption spectra for the four Ni coordination complexes. The inset shows the RIXS constant final state plots compared to the absorption K pre-edge region (dashed lines). Right panel: L_3-edge absorption spectra (black dashes) compared to RIXS constant incident energy plots following excitations from 1s to 3d (green lines) and to higher vacant orbitals (orange lines).

$1s \rightarrow 3d$ resonances with oxidation state are clearly visible. For the Ni(I) complex, there is one vacant *3d* orbital, and, accordingly, we only observe one $1s \rightarrow 3d$ resonance. For Ni(II), there is either a single vacant *3d* orbital (low-spin) or a pair of degenerate *3d* orbitals (high-spin); again, we see only a single $1s \rightarrow 3d$ resonance. In contrast, two $1s \rightarrow 3d$ resonances are observed for the Ni(III) complex. This is consistent with at least some $3d^7$ character in the ground state configuration. Here, the Ni site has approximately tetragonal symmetry, and the low-spin (S = 1/2) configuration yields one unoccupied $3d_{x^2-y^2}$ orbital and a half-filled $3d_{xy}$ orbital. These features are nearly invisible in the transmission spectrum.

Traversing the contour plots parallel to $\Omega - \omega$ at a fixed excitation energy Ω yields "energy loss" spectra that involve the same final states as in $2p \rightarrow 3d$ ($L_{2,3}$) absorption spectroscopy (Fig. 3). In this case, exciting the $1s \rightarrow 3d$ intermediate resonance of the Ni(I) complex yields final states with a $2p^5 3d^{10}$ configuration. The "L_3" energy loss spectrum does not show any splitting because of the filled *3d* shell. Within the experimental resolution, a symmetrical peak is also observed for low-spin Ni(II). In contrast, the high-spin Ni(II) and low-spin Ni(III) L_3 energy loss spectra exhibit asymmetries because of multiplet structure. These features arise from (*2p*,*3d*) and (*3d*,*3d*) Coulomb and exchange interactions [6]. Additional structures arise from orbital energy splittings in the case of Ni(III). Multiplet splitting yields information on the valence and spin state of the metal center, and various L-edge studies have used these features to characterize metal centers [7]. Specifically, in L-edge spectroscopy, the high-energy shoulder in the L_3 line has been used as a diagnostic of high-spin Ni(II) in metalloproteins, while a low-energy peak ascribed to Ni(III) has been used to characterize Ni oxides. This low-energy feature can be seen in the Ni(III) $\Omega - \omega$ spectrum (Fig. 3). (Since this sample exhibits two $1s \rightarrow 3d$ bands, we show two constant incident energy plots, taken at the peak of each resonance.)

The contour plots show resonances at energies higher than the primary $1s \rightarrow 3d$ excitations. These features involve antibonding molecular orbitals with some metal character. For example, in the [PhT^{tBu}]Ni(I)CO complex, there is a low-lying CO π^* orbital that mixes with Ni *3d* and *4p* orbitals.

The sensitivity of the *1s2p* RIXS spectroscopy is high enough for applications in biocatalysis. We investigated the active site of the [NiFe] hydrogenase *Desulfovibrio gigas* that catalyzes the reversible reaction $H_2 \leftrightarrow 2H^+ + 2e^-$. The line plot in Fig. 4 shows the pre-edge structure extracted from the *1s2p* RIXS plane of the enzyme as isolated and reduced by adding dithionite. The shift of the resonance to lower energies indicates reduction of the Ni in the active site.

Acknowledgments

This work was supported by National Institutes of Health (NIH) Grant No. GM-44380 and by the U.S.

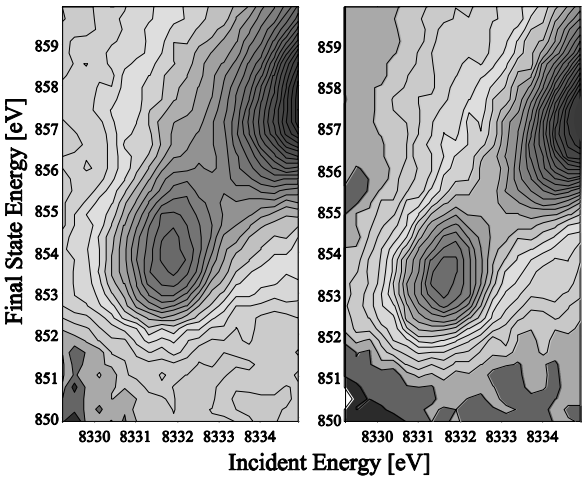

FIG. 4. Separated 1s to 3d resonances obtained from the RIXS plane in [NiFe] hydrogenase Desulfovibrio gigas.

Department of Energy (DOE), Office of Biological and Environmental Research. Use of the APS was supported by the DOE Office of Science, Office of Basic Energy Sciences (BES), under Contract No. W-31-109-ENG-38. BioCAT is a NIH-supported Research Center RR-08630. The Advanced Light Source (ALS, LBNL) and Stanford Synchrotron Radiation Laboratory (SSRL) are supported by the DOE BES.

References

[1] W. A. Caliebe, C. C. Kao, J. B. Hastings, M. Taguchi, T. Uozumi, and F. M. F. de Groot, Phys. Rev. B **58**, 13452-13458 (1998).

[2] P. Glatzel, U. Bergmann, W. Gu, H. Wang, S. Stepanov, B. S. Mandimutsira, C. Riordan, C. P. Horwitz, T. Collins, and S. P. Cramer (submitted).

[3] P. Carra; M. Fabrizio, and B. T. Thole, Physical Review Letters **47**, 3000-3003 (1995); and A. Kotani and S. Shin, Rev. Mod. Phys. **73**, 203-246 (2001).

[4] G. B. Bunker, T. Irving, E. Black, K. Zhang, R. Fischetti, S. Wang, and S. Stepanov, Synchrotron Radiation Instrumentation 10th U.S. National Conference **16** (1997).

[5] U. Bergmann and S. P. Cramer, SPIE Proceedings **3448**, 198-209 (1998).

[6] J. C. Slater, *Quantum Theory of Atomic Structure* (McGraw-Hill, New York, NY, 1960).

[7] F. M. F. de Groot, Chem. Rev. **101**, 1779-1808 (2001).